Nov 10th, 12:00 AM - 12:00 AM

Reduced Order Models for Profiled Steel Diaphragm Panels

G. Bian

S. Torabian

B. W. Schafer

Wei-Wen Yu International Specialty Conference on Cold-Formed Steel Structures
Baltimore, Maryland, U.S.A, November 9 & 10, 2016

Reduced Order Models for Profiled Steel Diaphragm Panels

G. Bian[1], S. Torabian[2], B.W.Schafer[3]

Abstract

The objective of this paper is to provide progress on development and validation of reduced order models for the in plane strength and stiffness of profiled steel panels appropriate for use in structural models of an entire building. Profiled steel panels, i.e, metal deck, often serve as a key distribution element in building lateral force resisting systems. Acting largely as an in-plane shear diaphragm, metal deck as employed in walls, roofs, and floors plays a key role in creating and driving three-dimensional building response. As structural modeling evolves from two-dimensional frameworks to fully three-dimensional buildings, accurate and computationally efficient models of profiled steel panels are needed. Three-dimensional building response is increasingly required by ever-evolving structural standards, particularly in seismic design, and structural efficiency demands that the benefits of three-dimensional response be leveraged in design. Equivalent orthotropic plate models provide a potential reduced order model for profiled steel panels that is investigated in this paper. A recent proposal for the rigidities in such a model are assessed against shell finite element models of profiled steel panels. In addition, the impact of discrete connections and discrete panels, as occurs in an actual roof system, are assessed when applying these reduced order models. Extension of equivalent orthotropic plate models to elastic buckling and strength, in addition to stiffness, both represent work in progress, but initial results are provided. Examples show that equivalent orthotropic plate models must be used with care to yield useful results. This effort is an initial step in developing efficient whole building models that accurately incorporate the behavior of profiled steel panels as diaphragms.

[1] Ph.D. student, Department of Civil Engineering, Johns Hopkins University, Baltimore, MD, 21218. <bian@jhu.edu>
[2] Assistant Research Professor, Department of Civil Engineering, Johns Hopkins University, Baltimore, MD, 21218. <torabian@jhu.edu>
[3] Professor, Department of Civil Engineering, Johns Hopkins University, Baltimore, MD, 21218. <schafer@jhu.edu>

Introduction

Profiled steel panels, i.e., metal deck, are roll-formed from thin steel sheet and can result in simple corrugated shapes or relatively complex longitudinal profiles with additional transverse features such as embossments. These panels serve as the walls and roof in many metal buildings, see Figure 1, and form an integral component of common floor systems in a wide variety of buildings. Under lateral loads the panels play a particularly important role as a distribution element, one in which the in-plane shear behavior of the panel is paramount. A typical profiled steel panel roof is illustrated in Figure 1. When distributing lateral load this system acts as a diaphragm, with all elements in the system contributing: panel, panel inter-connections, joists, joist-to-panel connections, primary framing, and framing-to-panel connections.

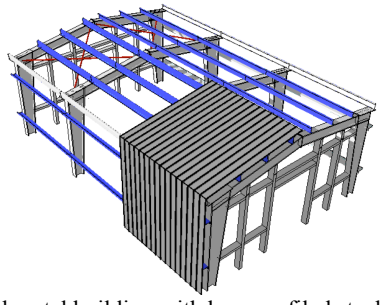

Figure 1. Typical metal building with bare profiled steel panel diaphragms

Traditionally, the lateral (e.g., seismic) behavior of buildings has been engineered by examining the two-dimensional (2D) behavior of the lateral force resisting systems in the primary frames of a building. Increasingly, this is becoming inadequate as (a) experimental evidence mounts that response is largely three-dimensional (3D), (b) efficiencies demand the full 3D response be understood, (c) more complex building geometries are being pursued, and (d) advances in idealizing loads creates more precise 3D demands to be considered. In addition, due to advancements in Building Information Modeling it is now more common to have 3D building models. As a result, it is highly desirable for the engineer to develop 3D structural models; however, while such models can now be more readily created and their need is real, with all details included such models can be prohibitively costly to run, particularly given the myriad of load cases. Thus, we seek the advancement of accurate reduced order models that can be employed in 3D structural models, for modeling diaphragms with profiled steel panels. The focus of this paper is on the reduced order modeling of the panel itself with additional examination of the panel connections. Future work intends to extend the effort to the complete system of Figure 1.

In-plane elastic behavior of profiled steel panels

The in-plane behavior of profiled steel panels is critical for its action as a diaphragm. Even in the linear elastic range the mechanics involved in the in-plane deformations are interesting. Consider a trapezoidal corrugated panel under in-plane actions as illustrated in Figure 2, (a) perpendicular to the corrugations significant bending occurs and the panel is quite weak with little Poisson effect, (b) parallel to the corrugations the deformations are largely axial with some Poisson effect, (c) under in-plane shear edge (warping) conditions of the panel become important and bending of the corrugations occur.

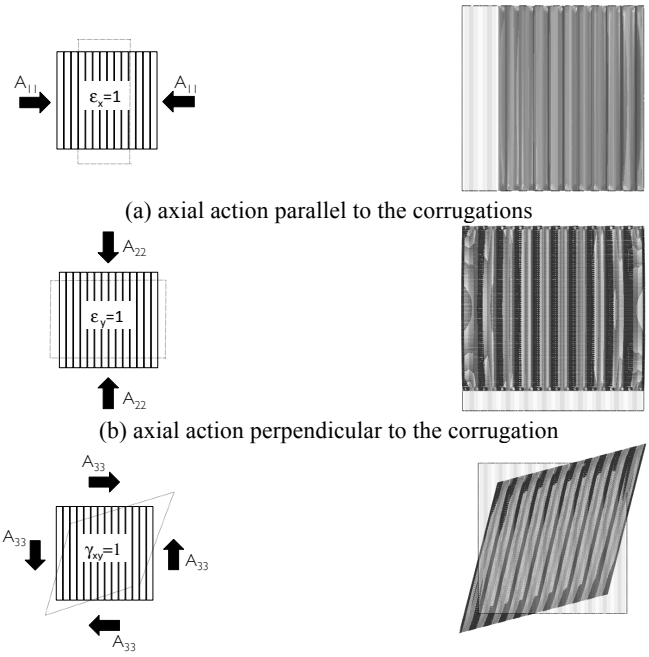

(a) axial action parallel to the corrugations

(b) axial action perpendicular to the corrugation

(c) in-plane shear

Figure 2. In-plane loading and FE predicted elastic deformations for profiled steel panel

Engineering models of a profiled steel panel typically cannot include the details of the corrugation and instead must resort to an equivalent flat plate. Due to the strongly different stiffness parallel and perpendicular to the corrugations a natural choice is an equivalent orthotropic flat plate as detailed in the following section.

Equivalent orthotropic flat plate for corrugated steel panel

The notion of employing an equivalent orthotropic flat plate to simulate a corrugated plate has long been used in engineering. Typically, out-of-plane bending behavior is of primary interest as opposed to in-plane behavior and early work such as Easley and Mcfarland (1969) investigated equivalent flexural rigidities. More recently Samanta and Mukhopadhyay (1999) re-examined the problem and developed closed-form expressions for the orthotropic plate rigidities for both out-of-plane (flexure) and in-plane (extension and shear). This was followed by Xia et al. (2012), who expanded on the earlier work including correcting some assumptions, and derived a set of plate rigidities for equivalent orthotropic plates to model the elastic stiffness of a corrugated plate.

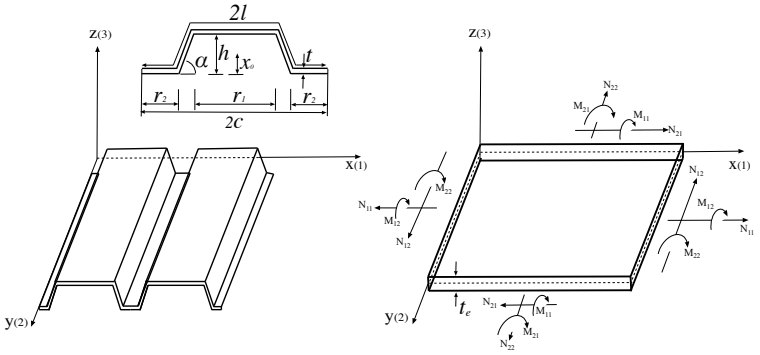

(a) profiled steel panel (b) equivalent orthotropic plate

Figure 3. Coordinates and basic dimensions

Central to the work of Xia et al. (2012) and studied here is the conversion of a corrugated plate such as Figure 3(a) into that of an equivalent orthotropic flat plate Figure 3(b). The rigidities that define the equivalent flat plate connect forces and moments on the equivalent plate to strains and curvatures, via:

$$\begin{Bmatrix} \overline{N_x} \\ \overline{N_y} \\ \overline{N_{xy}} \\ \overline{M_x} \\ \overline{M_y} \\ \overline{M_{xy}} \end{Bmatrix} = \begin{bmatrix} \overline{A_{11}} & \overline{A_{12}} & 0 & 0 & 0 & 0 \\ \overline{A_{12}} & \overline{A_{22}} & 0 & 0 & 0 & 0 \\ 0 & 0 & \overline{A_{66}} & 0 & 0 & 0 \\ 0 & 0 & 0 & \overline{D_{11}} & \overline{D_{12}} & 0 \\ 0 & 0 & 0 & \overline{D_{12}} & \overline{D_{22}} & 0 \\ 0 & 0 & 0 & 0 & 0 & \overline{D_{66}} \end{bmatrix} \begin{Bmatrix} \overline{\varepsilon_x} \\ \overline{\varepsilon_y} \\ \overline{\gamma_{xy}} \\ \overline{\kappa_x} \\ \overline{\kappa_y} \\ \overline{\kappa_{xy}} \end{Bmatrix} \tag{1}$$

where the overbars in Eq. (1) indicate they are for the equivalent plate not the original corrugated plate. In addition, membrane-bending coupling has been ignored. Xia et al (2012) completed a series of energy solutions that exercise unit strains on the corrugated plate and developed the plate rigidities directly based on the geometry and traditional beam mechanics for the in-plane terms and Kirchoff plate theory for the flexural terms. The developed expressions are provided in Table 1 along with additional relevant plate rigidities.

Table 1: Plate Rigidities

	uniform flat plate		direct definition
Rigidity	isotropic[a]	orthotropic[b] (eng. constants)	orthotropic[c] (Xia et al. 2012)
$\overline{A_{11}}$	$\frac{Et}{1-\nu^2}$	$\frac{E_1 t_e}{1-\nu_{12}\nu_{21}}$	$\frac{2c}{\frac{I_1(1-\nu^2)}{Et}+\frac{12I_2(1-\nu^2)}{Et^3}}$
$\overline{A_{22}}$	$\frac{Et}{1-\nu^2}$	$\frac{E_2 t_e}{1-\nu_{12}\nu_{21}}$	$\nu\overline{A_{12}}+\frac{l}{c}\left(\nu-\nu^2\right)\frac{Et}{1-\nu^2}$
$\overline{A_{12}}$	$\nu\frac{Et}{1-\nu^2}$	$\nu_{12}\frac{E_2 t_e}{1-\nu_{12}\nu_{21}}$	$\nu\frac{2c}{\frac{I_1(1-\nu^2)}{Et}+\frac{12I_2(1-\nu^2)}{Et^3}}$
$\overline{A_{66}}$	Gt	$G_{12}t_e$	$\frac{l}{c}Gt$
$\overline{D_{11}}$	$\frac{Et^3}{12(1-\nu^2)}$	$\frac{E_1 t_e^3}{12(1-\nu_{12}\nu_{21})}$	$\frac{c}{l}\frac{Et^3}{12(1-\nu^2)}$
$\overline{D_{22}}$	$\frac{Et^3}{12(1-\nu^2)}$	$\frac{E_2 t_e^3}{12(1-\nu_{12}\nu_{21})}$	$\frac{1}{2c}\left[I_2\frac{Et}{1-\nu^2}+I_1\frac{Et^3}{12(1-\nu^2)}\right]$
$\overline{D_{12}}$	$\nu\frac{Et^3}{12(1-\nu^2)}$	$\nu_{12}\frac{E_2 t_e^3}{12(1-\nu_{12}\nu_{21})}$	$\nu\frac{c}{l}\frac{Et^3}{12(1-\nu^2)}$
$\overline{D_{66}}$	$\frac{Gt^3}{12}$	$\frac{G_{12}t_e^3}{12}$	$\frac{l}{c}\frac{Gt^3}{12}$
	$G=E/2(1+\nu)$	$\nu_{12}E_2=\nu_{21}E_1$	

a. uniform plate, thickness t, material properties E and ν, note $G=E/2(1+\nu)$.

b. uniform orthotropic plate, thickness t_e, properties $E_1,E_2,\nu_{12},\nu_{21},G_{12}$, note $\nu_{12}E_2=\nu_{21}E_1$

c. E, ν, G, t properties of original corrugated plate, c and l properties of section per Figure 2, $I_1=\int_0^{2l}\left(\frac{dx}{ds}\right)^2 ds$ and $I_2=\int_0^{2l} z^2 ds$. Explicit expressions provided for common cases below.

An equivalent isotropic flat plate can only match two rigidities of the actual plate, and is therefore of limited use. Interestingly, an equivalent orthotropic flat plate, with uniform thickness, cannot match all of the 8 directly defined rigidities from Xi et al. (2012) either. While multi-purpose finite element software such as ABAQUS (2012) allows the plate rigidities of Eq. 1 to be defined directly most commercial structural engineering software does not, and at best allows the orthotropic engineering constants: E_1, E_2, ν_{12}, ν_{21}, G_{12} and an equivalent thickness, t_e, to be defined. Therefore, in addition to the Xia et al. (2012) expressions, the engineering constants that provide best agreement are also useful. The selection is not unique and depends on what quantities the engineer/analyst desires to match. For diaphragms the in-plane quantities are of the greatest prominence, therefore one set of solutions is to match the Xia et al. 2012 in-plane rigidities to an explicitly defined flat plate with orthotropic material one as follows:

$$E_2 = E \text{ decided a priori} \tag{2}$$

$$\frac{E_1}{E_2} = \frac{\overline{Xia\,A_{11}}}{\overline{Xia\,A_{22}}} \rightarrow E_1 = \frac{\overline{Xia\,A_{11}}}{\overline{Xia\,A_{22}}} E_2 \tag{3}$$

$$\nu_{12}E_2 = \nu_{21}E_1 \rightarrow \nu_{21} = \nu_{12}E_2 / E_1 \text{ to maintain 12=21 terms} \tag{4}$$

$$\frac{E_1 t_e}{1-\nu_{12}\nu_{21}} = \overline{Xia\,A_{11}} \rightarrow t_e = \overline{Xia\,A_{11}} \frac{1-\nu_{12}\nu_{21}}{E_1} \tag{5}$$

$$\nu_{12}\frac{E_2 t_e}{1-\nu_{12}\nu_{21}} = \overline{Xia\,A_{12}} \rightarrow t_e = \overline{Xia\,A_{12}} \frac{1-\nu_{12}\nu_{21}}{\nu_{12}E_2} \tag{6}$$

$$\overline{Xia\,A_{11}} \frac{1-\nu_{12}\nu_{21}}{E_1} = \overline{Xia\,A_{12}} \frac{1-\nu_{12}\nu_{21}}{\nu_{12}E_2} \rightarrow \nu_{12} = \frac{\overline{Xia\,A_{12}}}{\overline{Xia\,A_{11}}} \frac{E_1}{E_2} \tag{7}$$

$$G_{12}t_e = \overline{Xia\,A_{66}} \rightarrow G_{12} = \overline{Xia\,A_{66}} / t_e \tag{8}$$

Note the Xia et al. 2012 expressions include the integrals I_1 and I_2 defined in the footnote to Table 1. For geometries common to steel panels, explicit form of these integrals are:

$$I_1 = 2c - 2h\frac{\cos\alpha(1-\cos\alpha)}{\sin\alpha} \tag{9}$$

$$I_2 = \frac{2((h-x_0)^3 + x_0^3)}{3\sin\alpha} + r_1(h-x_0)^2 + 2r_2 x_0^2 \tag{10}$$

where $x_0 = \frac{r_1 h}{2l} + \frac{h^2}{2l\sin\alpha}$, c, h, α, r_1, r_2, and l, are defined in Figure 3.

Validation of equivalent in-plane stiffness for corrugated panels

To validate the in-plane equivalent orthotropic plate rigidities of Xia et al. (2012) and address an ambiguity in the edge boundary conditions a series of shell finite element models of square (1016 mm × 1016 mm) corrugated plates (c=50.8 mm, r=25.4 mm, l=61.3 mm, t=6.35 mm, E=210000N/mm^2, α=45^o) were developed in ABAQUS using S4R elements. The models were exercised with in-plane actions consistent with Figure 2: ε_x=constant, ε_y=constant, and γ_{xy}=constant applied as perimeter displacements. These actions define u_x and u_y for the perimeter, but u_z, θ_x, θ_y, and θ_z are undefined and four cases from supported-clamped through out-of-plane free as illustrated in Figure 4 are considered. The stiffness predicted by Xia et al. (2012) is compared with the shell FE model in Table 2.

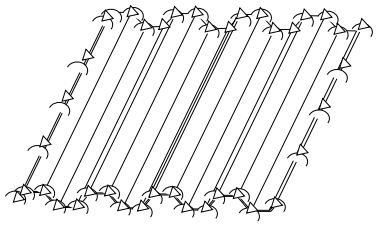

Case 1: Perimeter *supported* out-of-plane (u_z=0) and *clamped* (θ_x=θ_y=θ_z=0)

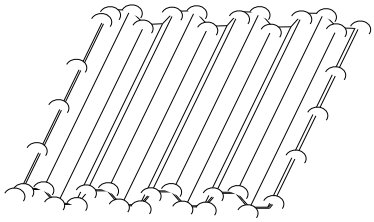

Case 2: Perimeter free out-of-plane but *clamped* (θ_x=θ_y=θ_z=0)

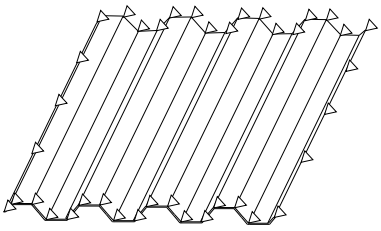

Case 3: Perimeter *supported* out-of-plane (u_z=0) but free to rotate

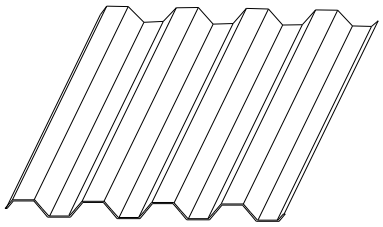

Case 4: Perimeter free, only in-plane applied DOF applied

Figure 4. Boundary conditions for corrugated plate with applied in-plane actions

From Table 2 we can observe that under the right boundary conditions the expressions of Xia et al. (2012) are in excellent agreement with the full corrugated plate shell FE model. The rigidity aligned with the corrugations (A_{22}) is not sensitive to the boundary conditions; however, the rigidity perpendicular to the corrugations (A_{11}, A_{12}) is sensitive. The source of this sensitivity is the eccentricity between the centroid in the transverse direction and the location

where transverse displacements are applied, i.e. the bottom of the corrugation as illustrated in Figure 5. The Xia et al (2012) solution agrees best with the assumption of no out-of-plane support (Case 4), thus the engineer must understand that this eccentricity is embedded in the expressions and not account for it a second time in their modeling. Interestingly, the in-plane shear rigidity expressions (A_{66}) agrees best with cases 1 and 3, where the entire perimeter is supported out-of-plane. If this out-of-plane support is removed then the eccentricity effect is activated and the shear stiffness reduces; however Xia et al. (2012) does not account for this effect in shear. Thus, the engineer must be aware that the Xia et al. (2012) expressions may modestly overestimate shear stiffness of the panel.

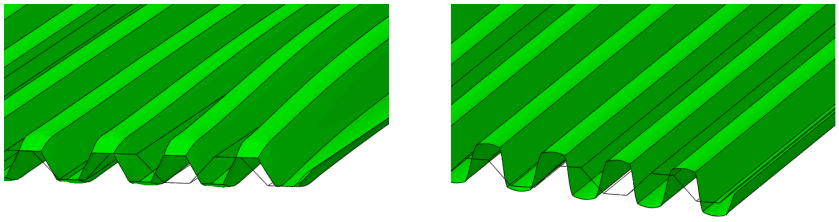

Case 1: Perimeter *supported* out-of-plane (u_z=0) and *clamped* (θ_x=θ_y=θ_z=0)

Case 4: Perimeter free, only in-plane applied DOF applied

Figure 5. Deformation in FE model under transverse strain

Table 2. Comparison between FEM results and equivalent stiffness

		Corrugated plate shell FE model / $\overline{A_{ij}}$			
	Xia et al. (2012) / Table 1 (N/mm)	Case I Supported-Clamped edge	Case 2 Clamped edge	Case 3 Supported edge	Case 4 "Free" edge
$\overline{A_{22}}$	163910	0.99	0.98	0.99	0.98
$\overline{A_{11}}$	4051	1.38	1.11	1.21	0.97
$\overline{A_{12}}$	1215	1.57	1.29	1.19	0.98
$\overline{A_{66}}$	42489	1.00	0.96	1.00	0.92

Note: if direct rigidities cannot be modeled Eq. (2)-(8) provide E_1=161 MPa, E_2=203500 MPa, ν_{12}=0.00024, ν_{21}=0.3, G_{12}=91170 MPa, t_e=0.286 mm and have been validated to match Xia et al (2012) in the model

Impact of discrete connection points and panels on diaphragm stiffness

The previous section validates the in-plane equivalent orthotropic model for an isolated panel under idealized boundary conditions. Actual diaphragms are composed of multiple discrete panels that are connected to one another and to joists and perimeter framing. This section examines the impact of these details on the realized diaphragm stiffness and the accuracy of the equivalent orthotropic plate model.

Recent testing by Tremblay and Rogers (2004) motivated the geometry studied here. Specifically, an example diaphragm ~ 6 m x 3m in plan employing the P-3615 Canam profile as illustrated in Figure 6 is studied. The models in this section do not include the stiffness of fasteners connecting panels or connecting to the frame, but rather treats these locations as discrete constraint points. Thus, the impact of localized forces on the panels is introduced, but the impact of the fastener stiffness is isolated from these effects. This provides an upperbound approximation of the stiffness and one that focuses entirely on the accuracy of the panel modeling. Unlike Figure 2, shear in this model is applied in the same manner as in testing with the boundary conditions as illustrated in Figure 6(c).

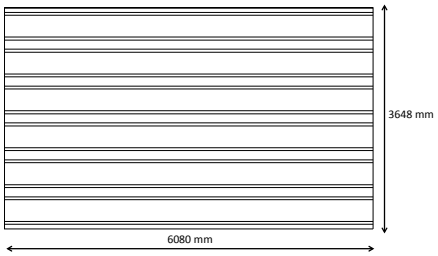

(a) Overall panel dimension

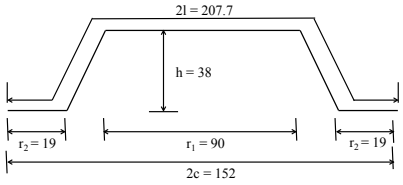

(b) Cross-section dimensions (mm)

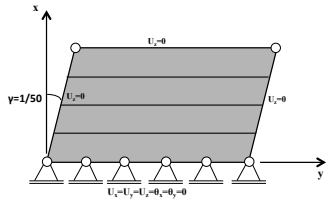

(c) boundary conditions and loading

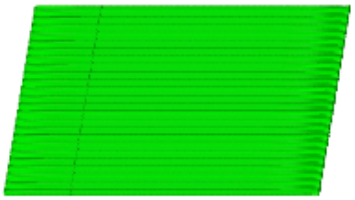

(d) typical response for one large panel

Figure 6. Geometry of studied diaphragm

Table 3. Elastic shear stiffness for different panels, connection points, and plate models

		FE model (1) corrugations in model	FE model (2) ortho. plate Xia et al.	FE model (3) ortho. plate E_1, E_2, etc.
Panels	Perimeter conn.	S_{FE1} (N/mm)	S_{FE2}/S_{FE1}	S_{FE2}/S_{FE1}
One large panel	Every node	52224	1.0	1.0
One large panel	304 mm o.c.	16676	0.2	0.2
Four discrete panels[a]	Every node	37119	1.1	1.1
Four discrete panels[a]	304 mm o.c.	14687	0.2	0.2

[a] modeling of discrete panels also includes three interior connection lines

The results, provided in Table 3, indicate that only under idealized edge boundary conditions is the equivalent orthotropic plate model adequate. With discrete connection points even though the global deformation is shear the extremely weak stiffness in the transverse corrugation direction (A_{11} rigidity direction) creates significant local deformations that greatly decrease the overall stiffness. Localized forces (connection points) that are parallel to the corrugation (A_{22} rigidity direction) do not show similar sensitivity, so the sidelap connections of the model with four discrete panels are not problematic (locally they engage A_{22} rigidity), rather the perimeter connections that are transverse to the corrugations (in the short direction of the model) create the difficulties Therefore, engineers must be careful when using equivalent orthotropic plate models and recognize that the derived values do not apply directly to panels with discrete connections transverse to the corrugations, a significant limitation.

Accuracy of elastic buckling solutions with orthotropic plate models

The elastic buckling response of profiled steel panels is an important consideration in their design. For geometric nonlinear analysis of buildings, as is often pursued for predicting ultimate response, the elastic buckling of the panels is indicative of the potential large deformations the panel may undergo. Elastic shear buckling is known to be sensitive to the details of the profile, here we investigate to what extent an equivalent orthotropic plate can still capture these geometric nonlinearities by investigating the eigenbuckling modes of the panel from the previous section (i.e., Figure 6) with explicit FE models of the corrugations compared with equivalent orthotropic plate models.

Selected elastic shear buckling loads and corresponding mode shapes for the three studied models are provided in Table 4 and Figure 7. The elastic buckling results indicate that panel shear buckling is the lowest buckling mode, but the equivalent orthotropic plate models are inadequate for accurate prediction. The model based on the direct rigidities (including D_{ij}) from Xia et al. (2012) is slightly better than the model based on the use of general engineering parameters (E_1, E_2, etc.) that were fit to the in-plane rigidities (A_{ij}). However, the error is so large that the engineer must use the equivalent plate model with great care for nonlinear analysis. It is interesting to note that in the actual profiles (FE model 1) the buckling mode is not influenced by local edge conditions until the 13th mode, fully 1.5 times higher than the lowest (first) mode.

Table 4. First six elastic buckling modes for panel of Figure 6 modeled as 4 separate discrete panels connected every 300 mm o.c. at the perimeter and between panels

	FE model (1) corrugations in model		FE model (2) ortho. plate Xia et al.		FE model (3) ortho. plate E_1, E_2, etc.	
mode	V_{cr1} (kN)	notes	V_{cr2} (kN)	notes	V_{cr3} (kN)	notes
1	99	Panel[(a)]	32	Panel[(c)]	26	Panel
3	100	Panel	33	Panel	26	Panel
13	147	Panel	46	Panel	39	Panel
15	148	Panel+Edge[(b)]	50	Panel	41	Panel
21	152	Edge	73	Panel	58	Panel

Note: (a), (b), (c), see Figure 7 for corresponding buckling modes.

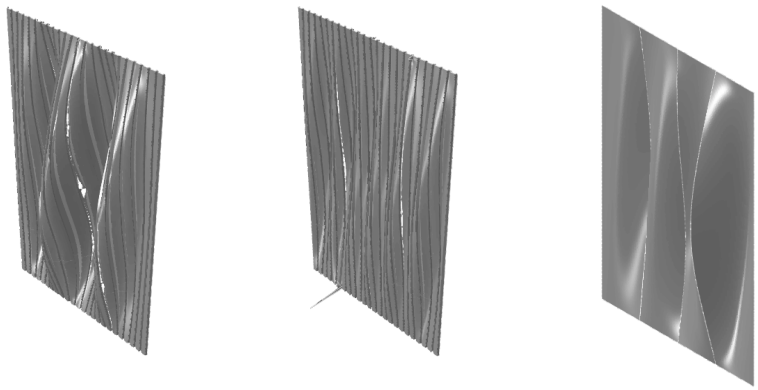

(a) mode 1, FE model 1 (b) mode 15, FE model 1 (c) mode 1, FE model 2

Figure 7 Selected elastic buckling modes in shear from models

Impact of panel yielding on diaphragm stiffness and strength

Finite element collapse analyses of four different shell finite element models with explicitly modeled profiles were conducted to study the impact of having discrete panels with discrete connections on their collapse behavior. We employed von Mises yield criteria with isotropic hardening and an elastic perfectly plastic stress-strain curve with F_y=345 MPa and E=203,500 MPa. Loading is the same as Figure 6. Four cases are studied (a) the panel is modeled as a single continuous corrugated panel and the perimeter is fully connected, (b) the panel is modeled as 4 discrete panels and the perimeter is fully connected, (c) the panel is modeled as a single panel and the perimeter is connected at 304 mm o.c., and (d) the panel is modeled as 4 discrete panels and the perimeter is connected at 304 mm o.c. Basic shear deformation-force results are provided in Figure 8 and indicate that in the idealized case the perimeter connection has a stronger influence on decreasing the stiffness and strength than the introduction of discrete panels. Additional study is needed including comparison to equivalent orthotropic plate models, but the shell finite element models are able to capture significant variations in the stiffness and strength as a function of expected details and results vary by as much as a factor of five indicating the importance of practical details above and beyond the basic panel properties.

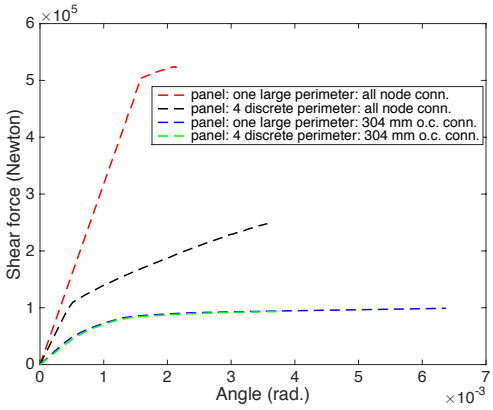

Figure 8 Nonlinear load-displacement curves in shear for studied models

Discussion

The design and behavior of profiled steel panels is complex and includes a number of issues not addressed in this work. Interested readers are referred to

AISI S310 (2013) for design standards, SDI DDM-04 (2015) for examples and additional information related to commonly available panels and connectors.

Reduced order models increase computational efficiency by reducing the degrees of freedom. Completed successfully, all important features are maintained and no compromise is required. The equivalent orthotropic plate reduced order model pursued here can accurately reproduce a variety of complex global stiffness behavior under idealized conditions, and with the explicit expressions of Xia et al. (2012) are relatively easy to implement. However, local features of the model are lost, and when applied in non-idealized conditions these features become important to the response and the accuracy of the model degrades. The application of equivalent orthotropic plate models must be done with care or the results can be overly conservative.

The need to create efficient building structural models is real, and the equivalent orthotropic plates studied herein have some potential, but may still represent too much computational overhead in some situations. Completely phenomenological models with as little as one degree of freedom are also needed and should be pursued in a manner consistent with codified design (strength and stiffness and post-peak response based on standards).

Conclusions

This paper examines the application of equivalent orthotropic plate models for profiled steel panels. Two methods for model implementation are explored: direct input of stiffness matrix rigidities, and equivalent thickness and material (E_1, E_2, etc.) properties. Under idealized boundary conditions the in-plane stiffness of both implementations of the equivalent orthotropic plate model are shown to have excellent agreement with shell finite element models of profiled steel panels. Relatively complex Poisson effects and bending effects are captured in the equivalent models under idealized conditions. However, under realistic conditions: discrete perimeter fastener spacing, or discrete numbers of panels the equivalent orthotropic plate model fails to capture the global in-plane shear response accurately. Global shear rigidity decreases when discrete fastening is introduced, but local rigidities in the equivalent orthotropic plate model, particularly transverse to the profiles, causes artificially large flexibility and results in stiffness that can be as little as 20% of the actual stiffness. Elastic buckling analysis further highlights this problem for equivalent orthotropic plate models. Reduced order models for profiled steel panels are needed for whole building analysis, equivalent orthotropic plate models provide one possible solution, but the analysis herein shows they must be used with care when exercised in realistic models of buildings.

Acknowledgments

Partial funding for this work was provided by the Steel Diaphragm Innovation Initiative (SDII) managed by the Cold-Formed Steel Research Consortium headquartered at Johns Hopkins University. SDII receives contributions from the American Institute of Steel Construction, the American Iron and Steel Institute, the Steel Deck Institute, the Steel Joist Institute, and the Metal Building Manufacturers Association. Any opinions, findings and conclusions or recommendations expressed in this material are those of the authors and do not necessarily reflect the views of the sponsors.

References

ABAQUS. ABAQUS/CAE User's Manual Version 6.12, Simulia. 2012.

AISI S310-13: AISI Standard "*North American Standard for the Design of Profiled Steel Diaphragm Panels*." American Iron and Steel Institute.

Briassoulis, D. (1986). Equivalent orthotropic properties of corrugated sheets. Computers & Structures, 23(2), 129-138.

Canam Group, (2007). Steel Deck Diaphragm Profile Manual. 2007.

Davies, J. M. (1976). Calculation of steel diaphragm behavior. Journal of the Structural Division, 102(ASCE# 12254).

Easley, J. T., & McFarland, D. E. (1969). "Buckling of light-gage corrugated metal shear diaphragms." *Journal of the Structural Division*, 95(7), 1497-1516.

Samanta, A., & Mukhopadhyay, M. (1999). "Finite element static and dynamic analyses of folded plates." *Engineering Structures*, 21(3), 277-287.

Steel Deck Institute, (2015) *Diaphragm Design Manual Fourth Edition.* 2015

Xia, Y., Friswell, M. I., & Flores, E. S. (2012). "Equivalent models of corrugated panels." *International Journal of Solids and Structures*, 49(13), 1453-1462.